

Numerical computation of the Schwarz function

Lloyd N. Trefethen

*School of Engineering and Applied Sciences, Harvard University,
29 Oxford St., Cambridge, MA, 02138, USA.

Corresponding author(s). E-mail(s): trefethen@seas.harvard.edu;

Abstract

An analytic function can be continued across an analytic arc Γ with the help of the Schwarz function $\mathbf{S}(z)$, the analytic function satisfying $\mathbf{S}(z) = \bar{z}$ for $z \in \Gamma$. We show how $\mathbf{S}(z)$ can be computed with the AAA algorithm of rational approximation, an operation that is the basis of the AAALS method for solution of Laplace and related PDE problems in the plane. We discuss the challenge of computing $\mathbf{S}(z)$ further away from Γ , where it becomes multi-valued.

Keywords: analytic continuation, Schwarz function, AAA approximation, AAALS method

MSC Classification: 30B40 , 35B60 , 41A20 , 65N35

1 Introduction

The Schwarz function for an analytic arc Γ is a beautiful and long-established idea. It is simply the analytic function $S(z)$ defined near Γ that takes the values $S(z) = \bar{z}$ for $z \in \Gamma$, and it holds the key to the continuation of analytic functions across Γ , as well as the continuation of related functions such as harmonic potentials and Helmholtz wavefields. The ideas go back in part to Schwarz in 1870 [22, pp. 150–151], Grave in 1895 [12], and Herglotz in 1914 [13, p. 305], and the function was given its name by Davis and Pollak in 1958 [6]. Two books have been published, by Davis [5] and Shapiro [24]. Yet the Schwarz function is not a widely known or widely used tool, and a reason for this may be that until recently, there has been no method available for computing it

2 Numerical computation of the Schwarz function

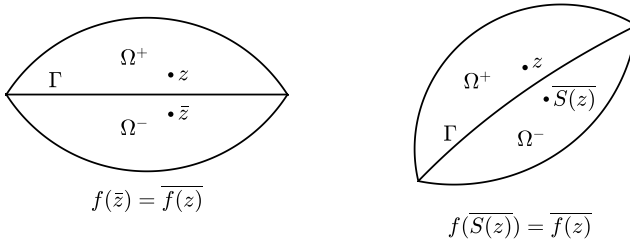


Fig. 1 On the left, the Schwarz reflection principle (Theorem 1) extends an analytic function that takes real values on a real interval across the interval from one half-plane to the other. On the right, the generalization by the Schwarz function $S(z)$ for reflection of an analytic function across an analytic arc Γ , again assuming it takes real values on Γ .

numerically, so it has played no role in numerical algorithms. Here we introduce such a method, based on AAA rational approximation. Examples of the method were shown earlier in [27] and [28].

2 The Schwarz function

The starting point of analytic continuation is the Schwarz reflection principle, whose simplest case is sketched on the left side of Figure 1. Let $\Omega \subseteq \mathbb{C}$ be a connected open set that is symmetric about \mathbb{R} , $\overline{\Omega} = \Omega$, and whose intersection with \mathbb{R} is a finite or infinite open interval Γ . (Here $\overline{\Omega}$ means the complex conjugate of Ω , not its closure.) We define $\Omega^+ = \{z \in \Omega : \text{Im}(z) > 0\}$ and $\Omega^- = \{z \in \Omega : \text{Im}(z) < 0\}$.

Theorem 1 Schwarz reflection principle. *Let Ω , Γ , Ω^+ and Ω^- be as defined above, and let f be analytic in the interior of Ω^+ and continuous on $\Omega^+ \cup \Gamma$, taking real values on Γ . Then the formula*

$$f(\bar{z}) = \overline{f(z)} \quad (1)$$

defines an analytic continuation of f to all of Ω .

Proof. Let f denote the function defined in all of Ω by (1), which makes sense as the two sides of the equation agree for $z \in \Gamma$ since z and $f(z)$ are real there. It is immediate that f is analytic in the interiors of Ω^+ and Ω^- (the Taylor series about two points z and \bar{z} are the same apart from conjugation of the coefficients) and that f is continuous throughout Ω . It remains only to show that f is analytic on Γ . This follows from a general principle involving analytic functions on adjacent domains that take the same continuous limit on an interface curve, which can be proved by a contour integral argument [20, p. 183]. ■

The Schwarz reflection principle is widely known and has applications to many situations. With the Schwarz function, we can generalize it to cases where

Γ is not a real segment but an analytic curve, as sketched on the right side of Figure 1. Let Γ be an analytic Jordan arc or Jordan curve, by which we mean the image in \mathbb{C} of the unit circle or an arc of the unit circle under a one-to-one analytic function with nonvanishing derivative. Consider the function

$$S(z) = \bar{z}, \quad z \in \Gamma. \quad (2)$$

(This may seem like the archetype of a nonanalytic function, but on an analytic curve as opposed to a domain with interior, $z \mapsto \bar{z}$ is analytic.) Like any other analytic function defined on a curve in \mathbb{C} , S can be analytically continued to a complex neighborhood of Γ , and this is the Schwarz function. In a word: $S(z)$ is the complex analytic function in a neighborhood of Γ that takes the values $S(z) = \bar{z}$ for $z \in \Gamma$. The point of S is that $z \mapsto \overline{S(z)}$ is the generalization to a general arc Γ of the reflection $z \mapsto \bar{z}$ when Γ is real.

We now explain how the analytic continuation works. Since S is analytic, it must extend to an analytic function on some neighborhood of Γ . Since $|d\overline{S(z)}/dz| = 1$ on Γ , it follows that in a sufficiently small neighborhood of Γ , $\overline{S(z)}$ maps a point z close to Γ on one side to a point close to Γ on the other side. This function $\overline{S(z)}$ is co-analytic, not analytic, but if we compose it with itself we get an analytic function—the identity:

$$\overline{\overline{S(z)}} = z. \quad (3)$$

To verify that (3) holds for z in a neighborhood of Γ , we note first that (2) implies that it holds for $z \in \Gamma$. It follows that on any neighborhood B of Γ such that S can be continued to B and then to $\overline{S(B)}$, the equality persists. Thus we see that the map $z \mapsto \overline{S(z)}$ is indeed a reflection sufficiently near Γ in the sense that its square is the identity. Such a map is called an involution. We make the following definition, sketched on the right side of Figure 1.

Definition 1 Given an analytic Jordan arc or Jordan curve Γ , a *reflection domain* for Γ is an open set $\Omega \subseteq \mathbb{C}$ containing Γ that is divided into two disjoint open sets Ω^- and Ω^+ by Γ and in which a single-valued analytic Schwarz function S for Γ can be defined that satisfies

$$\overline{S(\Omega^+)} = \Omega^-, \quad \overline{S(\Omega^-)} = \Omega^+, \quad (4)$$

and

$$\overline{\overline{S(z)}} = z, \quad z \in \Omega. \quad (5)$$

We can now state the generalization of the reflection principle.

Theorem 2 Reflection across an analytic curve. *Let Γ be an analytic Jordan arc or Jordan curve, let Ω be a reflection domain for Γ , and let f be analytic in the interior of Ω^+ and continuous on $\Omega^+ \cup \Gamma$, taking real values on Γ . Then the formula*

$$f(\overline{S(z)}) = \overline{f(z)} \quad (6)$$

4 Numerical computation of the Schwarz function

defines an analytic continuation of f to all of Ω .

Proof. The same as for Theorem 1, with the obvious changes. ■

Note that in both Theorems 1 and 2, we have supposed that f takes real values on Γ . If it takes imaginary values on Γ , the reflection formula adjusts to

$$f(\overline{S(z)}) = -\overline{f(z)}, \quad (7)$$

and there are similar elementary adjustments if Γ is another straight segment or a circular arc in \mathbb{C} . More generally, the situation in which f takes complex values along an analytic arc can be treated with the help of a second Schwarz function [24, Prop. 1.3], but we shall not consider this case.

Example: unit circle. If Γ is the unit circle, then $S(z) = z^{-1}$. Here we can take any annulus $r < |z| < r^{-1}$ with $r \in [0, 1)$ as a reflection domain. The choice $r = 0$ provides a reflection domain that is as large as possible, the punctured plane $0 < |z| < \infty$, but for choices of Γ other than a line or a circle, there may not be a maximal choice of Ω , because S will usually have branch points, as in the next example.

Example: ellipse. For any $\rho > 1$, define the ρ -ellipse E_ρ to be the image in the z -plane of the circle $|w| = \rho$ in the w -plane under the Joukowski map $z = (w + w^{-1})/2$. Geometrically, E_ρ is the ellipse with foci ± 1 whose semiminor and semimajor axis lengths sum to ρ . The Schwarz function for E_ρ is [5, p. 25]

$$S(z) = \frac{1}{2}(\rho^2 + \rho^{-2})z - \frac{1}{2}(\rho^2 - \rho^{-2})\sqrt{z^2 - 1}. \quad (8)$$

Note that S has a pair of branch points at ± 1 , and that otherwise, it is free of singularities in \mathbb{C} . As a reflection domain Ω for S , the obvious choice is to take \mathbb{C} minus a branch cut $[-1, 1]$, and also removing the reflection of $[-1, 1]$ in the ellipse, namely the segments $(-\infty, -a]$ and $[a, \infty)$ with $a = \frac{1}{2}(\rho^2 + \rho^{-2})$. However, other choices of branch cuts and reflection domains are also valid.

Besides the circle and ellipse, certain other domains have known Schwarz functions, such as parabolas and hyperbolas, as reported in [5]. However, there are not many such cases. A good deal of attention has been given to the study of so-called *quadrature domains*, which are domains for which the interior has a Schwarz function that is meromorphic, i.e., analytic apart from poles [9, 24]. These too are very special cases, as the nearly universal appearance of approximate branch cuts in calculations like those illustrated in Figures 2–5 of this paper testifies.

3 AAA approximation of the Schwarz function

In 2018 an algorithm for numerical rational approximation was published that is a step change from previously available algorithms, making it now possible to compute near-optimal approximations of many functions on many domains

in a fraction of a second on a laptop. This is the AAA algorithm, whose name derives from “adaptive Antoulas-Anderson.” The algorithm is a greedy iteration based on a barycentric representation of a rational function r with coefficients chosen at each iterative step via solution of a linear least-squares problem. We will not give details, which can be found in [18]. AAA has implementations in Matlab [8], Python [30], and Julia [7, 16], and its invocation in Matlab starts from the command

$$\mathbf{r} = \text{aaa}(\mathbf{F}, \mathbf{Z}) \quad (9)$$

where Z is a vector of sample points, typically a few hundreds or thousands, and F is a vector of corresponding function values. The output is a Matlab function handle corresponding to a rational function r satisfying

$$\frac{\|f - r\|}{\|f\|} \leq 10^{-13} \quad (10)$$

in the default mode of operation. Here $\|\cdot\|$ is the ∞ -norm over Z , which is typically an approximation to the ∞ -norm over a real or complex continuum of interest. The AAA rational approximation is not quite optimal for its degree, but its error is usually within a factor on the order of 10 of optimal. Another way to say it is that the AAA approximant often has degree about 10% greater than that of the minimal-degree approximation r satisfying (10).

Our proposed method for computing $S(z)$ is simply to apply the AAA algorithm to a discrete set Z of sample points along Γ , with function values $F = \overline{Z}$. The result is a rational function r that matches S to 13 digits of relative accuracy on Γ . (With extended-precision AAA implementations, such as are available in Julia, one can get more digits of accuracy.) The question then becomes, as z moves away from Γ , how much accuracy in $r(z) \approx S(z)$ is retained and for how far?

What almost always emerges from such computations is that r has strings of poles that approximate branch cuts, a phenomenon familiar in rational approximation and analyzed for Padé approximation by Stahl [25, 26] and for multipoint Padé approximation by Buslaev [2]. As our first illustration, the top-left panel of Figure 2 shows the poles of the AAA approximation to $S(z)$ for the case in which Γ is the ρ -ellipse with $\rho = 2$, discretized by 100 points. We see 23 poles lining up in $[-1, 1]$, nicely approximating a branch cut there. The figure also shows three arbitrarily chosen points z near Γ as orange dots and their reflections $\overline{r(z)} \approx \overline{S(z)}$ as green circles. The top-right panel of the figure repeats the same computation, except with Γ taken as just the upper half of the ellipse, which in principle has exactly the same Schwarz function. The same branch points are in evidence, but a different choice of branch cut. In addition to the 14 poles visible in the plot, there is also a pole off-scale at $\approx (4.4 - 7.4i) \times 10^7$, a numerical approximation to ∞ .

Where and how accurately does r approximate S ? As one indicator, following (5), we can compute $\overline{r(\overline{r(z)})}$ and see how close it comes to z itself at

6 Numerical computation of the Schwarz function

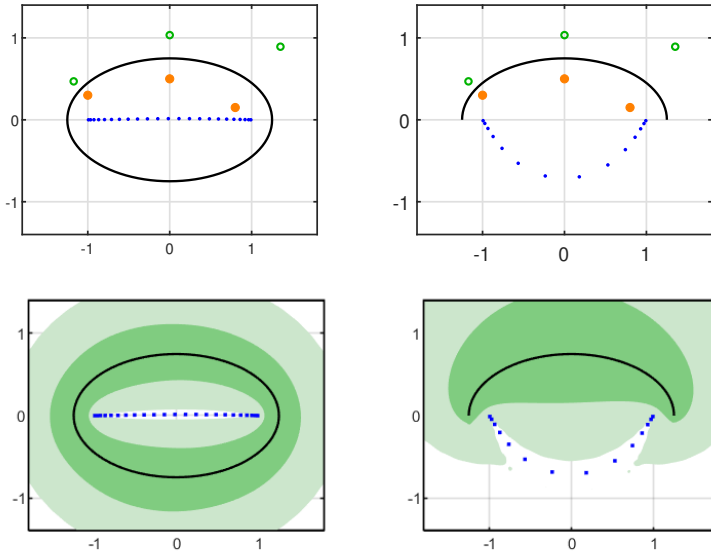


Fig. 2 In the first row, poles (blue) of AAA approximations to $S(z)$ for an ellipse and a half-ellipse. These computations took less than 0.01 s on a laptop. Both cases show a string of poles approximating a branch cut extending from -1 to 1 . In each image three orange points z have been selected and their reflections $\overline{r(z)} \approx \overline{S(z)}$ shown as green circles. In the second row, error indicators (11) of the approximations $r(z) \approx S(z)$. In the dark green region the accuracy is better than 10^{-8} , and in the light green region it is better than 10^{-1} .

various points $z \in \mathbb{C}$. The bottom row of Figure 2 applies this idea by filling in regions bounded by contours

$$|\overline{r(\overline{r(z)})} - z| = C \quad (11)$$

with $C = 10^{-8}$ (dark green) and $C = 10^{-1}$ (light green).¹ We will have more to say about these images in section 5.

Figure 3 applies the same computation to a pair of curves Γ for which $S(z)$ is not known analytically, defined in polar coordinates by a radius equal to $1 + 0.2 \sin(5\theta)$. Five branch cuts inside Ω and five more outside are in evidence, with a convincing reflection domain between them.

4 Singular and near-singular contours

Figure 4 shows four more examples of computed approximations to Schwarz functions. In the first row, Γ is an analytic curve as in our previous examples,

¹I am grateful to Keaton Burns for suggesting this method of visualization.

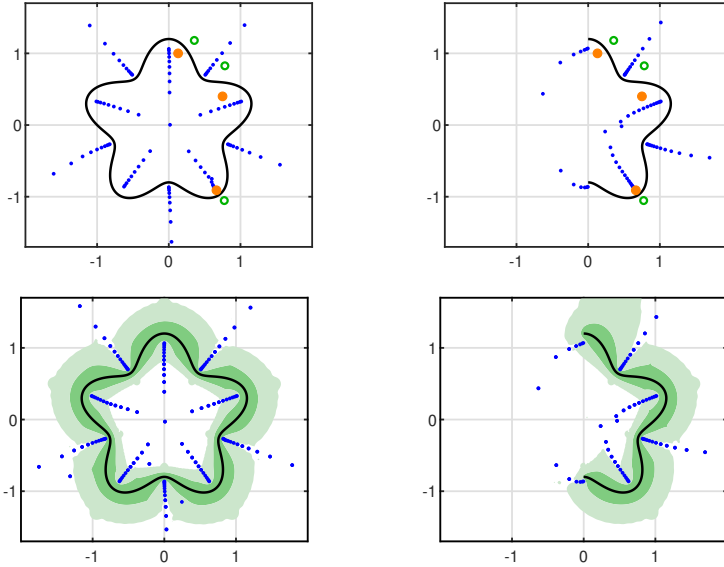


Fig. 3 Repetition of Figure 2 for a different pair of curves Γ .

whereas in the second row it has 1 and 6 singular points in the left and right images, respectively.

In the first image, Γ is a superellipse defined by the condition $x^6 + y^6 = 1$, discretized by 200 points. (In [5] and [6] an explicit formula for $S(z)$ is given for the curve defined by $x^4 + y^4 = 1$.) Besides the pole at the origin there are 68 further poles with four-fold symmetry (four of them off-scale in this image). The poles line up along a branch cut in the form of a cross with branch points approximately at $\pm 0.81 \pm 0.81i$.

The second image shows a domain with an inlet discretized in 300 points, a configuration where rational approximations are exponentially more powerful than polynomial approximations [28] (exponentially with respect to the inlet length-to-width ratio). There are 82 poles, six of them off-scale at $z \approx 2.1, 2.9, 4.3, 7.5, 17.5$, and 89.5 .

The third image introduces a singularity. Here Γ consists of an upper semicircle joined to a lower semicircle, so that at the junction at $z = 0$, Γ is C^1 but not C^2 . Each semicircle is discretized by 400 points exponentially clustered near $z = 0$, since poles will need to cluster there. Mathematically, there is one Schwarz function for the upper half and another for the lower half, both of them trivial since these are just semicircles. If we wish to think of a single global Schwarz function, then it will have two branches that are entirely independent, with no branch point linking the two. A global AAA rational approximation, however, is forced to choose a single-valued approximation, and one can see a curve of 68 poles dividing the semicircles (four of them off-scale) in addition to the two poles very close to $\pm i$. For this computation, which essentially involves

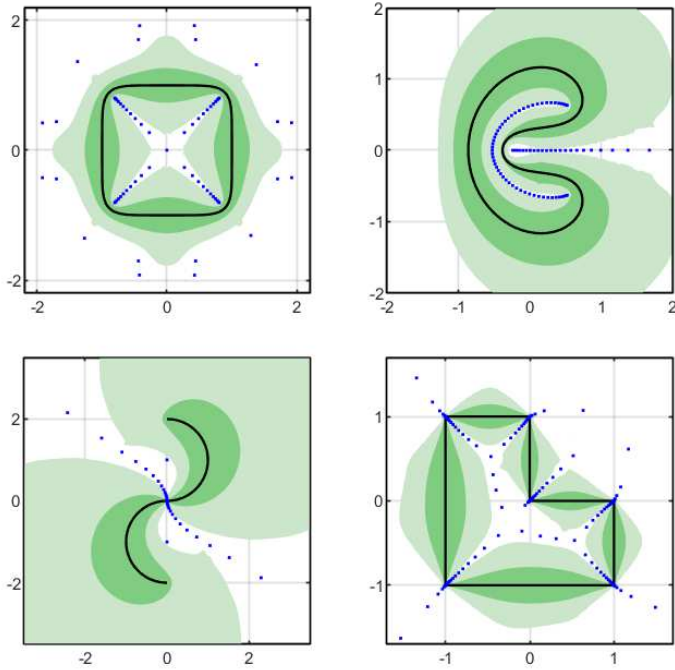


Fig. 4 Four more examples of numerically computed Schwarz functions. In the third image Γ has a singularity at $z = 0$, and in the fourth one, there are six singularities at the six corners. In both of these cases there are several mathematically independent branches of $S(z)$, which the rational approximations separate by strings of poles approximating branch cuts. For the final image the tolerance has been loosened to 10^{-8} and the dark green region shows accuracy 10^{-5} rather than the usual 10^{-8} .

a complex sign function, we found that for good results it was important to run the AAA algorithm with the 'sign' modification described in [29].

The fourth image shows an L-shaped region, each of whose six sides has been discretized by 300 points exponentially clustered at both ends. Whereas the other calculations each take on the order of 0.1 s on a laptop, this one requires 7 seconds because of the large number of poles, 361. In this configuration Γ is C^0 but not C^1 , putting it in the class of problems investigated by Newman in his study of rational approximation of $|x|$ on $[-1, 1]$ [21]. For such problems the convergence rate is root-exponential, i.e., with errors decreasing at the rate $\exp(-C\sqrt{n})$ as a function of degree n for some $C > 0$, and in this example we loosened the AAA tolerance from 10^{-13} to 10^{-8} . The contour level for the dark green region in the plot was correspondingly loosened from the usual 10^{-8} to 10^{-5} . Mathematically, the Schwarz function could be regarded as having six independent branches with no branch points, and again

the global rational approximation is forced to introduce approximate branch cuts, as is evident in the figure.

5 Multiple branches

In Figures 2–4, both the dark and light green regions can be interpreted as reflection domains as defined in section 2: to a certain numerical accuracy, the approximations $\overline{r(z)} \approx \overline{S(z)}$ reflect these domains across Γ into themselves.

The question presents itself, what can be said about the white regions in these plots? The first temptation is to suppose that these mark regions where the numerical approximation has simply failed to capture $S(z)$. However, the true situation is often better than this. Because of branch points, $S(z)$ is a multivalued function, and $r(z)$ is sometimes taking us with quite good accuracy to another branch.

We can see this effect in Figure 2, the example of the ellipse, where everything is known analytically. Suppose we start at the point $z = 1.3i$, which lies in the light green region, and apply $\overline{r(z)}$ several times. These are the values that result, showing just the alternation we hope for as z is reflected back and forth across Γ :

$$1.3i \rightarrow 0.3127i \rightarrow 1.3000i \rightarrow 0.3127i \rightarrow 1.3000i \rightarrow \dots \quad (12)$$

On the other hand if we start at $z = 3i$, which lies in the white region, this is what happens:

$$3i \rightarrow -0.4457i \rightarrow -1.1057i \rightarrow -0.4457i \rightarrow -1.1057i \rightarrow \dots \quad (13)$$

The initial reflection to $-0.4457i$ is extremely accurate, matching the exact value from (8) to 14 digits. Since the imaginary part is negative, however, this value has crossed the approximate branch cut of r . When r is applied to this new value, the number $-1.1057i$ matches the correct value for the *other* branch of S to 9 digits, as one can confirm by applying (8) with the sign of the square root negated. As a measure of this accuracy, Figure 5 repeats the lower half of Figure 2, but now, instead of measuring the error by (11), the plot colors regions according to

$$\min\{|r(z) - S_1(z)|, |r(z) - S_2(z)|\} = C, \quad (14)$$

where S_1 and S_2 are the two branches of the Schwarz function as given in (8). Now the blue ink covers a large area, except near the poles.

We thus see that AAA rational approximations $r(z)$ contain information that is easily interpretable in the green regions of Figures 2–4, and may also contain accurate information in parts of the white regions. Whether this information can be usefully utilized, or perhaps improved upon by the application

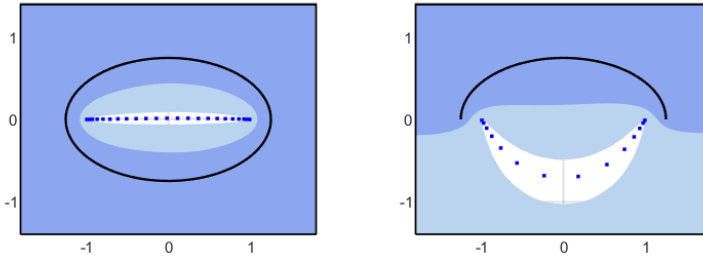


Fig. 5 Repetition of the bottom row of Figure 2 with (11) replaced by (14), so that the plot indicates deviation at each point from the closer of the two branches of the exact Schwarz function $S(z)$ of (8), and with colors changed from green to blue. Except along the approximate branch cut, r matches one or the other branch of $S(z)$ with good accuracy everywhere. The dark and light regions extend distances from the origin about 4000 and 1.5×10^7 on the left, 6 and 5000 on the right.

of other computational methods, remains to be seen. There is a small literature on numerical methods for tracking multivalued analytic functions, but it is not very advanced [10, 19, 23].

6 Discussion

My first motivation for computing the Schwarz function concerns the AAA-least squares (AAALS) method for solving 2D Laplace problems, which was invented by Stefano Costa [3]. For the basic example, consider the Dirichlet problem

$$\Delta u(z) = 0, \quad z \in \Omega, \quad u(z) = h(z), \quad z \in \Gamma, \quad (15)$$

where Γ is a Jordan curve bounding a Jordan domain Ω and h is a prescribed real function. In this numerical method, first one computes a AAA approximation $r \approx h$. This will normally have poles both inside and outside Γ , so its real part, which one might hope would solve the Laplace problem, will fail to be harmonic in Ω . The idea of the AAALS method is to discard the poles of r in Ω and use just the real and imaginary parts of the poles outside Ω to define a search space for approximating u by a linear least-squares calculation. The method is surprisingly fast and accurate in many cases, including, for example, on an L-shaped region as in Figure 4. So far, there is not much known to explain this success, or to delineate cases where the AAALS method fails, but the beginnings of a theory can be found in [28]. The key to taking the theory further probably lies with Schwarz functions.

The Schwarz function is also relevant to analytic continuation of solutions of more general PDEs problems, starting from the Hele-Shaw flow problem in fluid mechanics [4, 9, 14] and the Laplace equation in 3D [24]. Another important case is the Helmholtz equation $\Delta u + k^2 u = 0$ [1, 15, 17]. Generalizations of the AAALS method to some of these settings have proved effective, including axisymmetric 3D Laplace problems, Helmholtz equations [11], and

biharmonic/Stokes flow problems [31]. The present paper is offered partly with these situations in mind, and also because the topic of Schwarz functions is so interesting in its own right, so little studied, and potentially relevant to so many other problems of analytic continuation.

In closing, let us return for a moment to Figure 1. Comparing the two sides of the figure, one is reminded that the reflection across a general arc Γ effected by the Schwarz function, $z \mapsto \overline{S(z)}$, is a generalization of the reflection in the elementary case in which Γ is a line segment, $z \mapsto \bar{z}$. However, in its impact this is more than “just” a generalization because of the effect visible repeatedly in our figures: when a boundary Γ is curved, singularities of the Schwarz function are invariably introduced near Γ on the concave side. These singularities may determine the success or failure of subsequent numerical operations, and in particular, as shown in [28], they lead to rational approximations on non-convex domains being exponentially more efficient than polynomial ones. Thus rational approximation is both a good way to calculate Schwarz functions, and a motivation for wanting to do so.

Acknowledgments

I am happy to thank Keaton Burns, Stefano Costa, Kyle McKee, and Nicholas West for advice on this paper. Looking back, I am grateful for all I have learned about rational approximation over the years from Ed Saff.

References

- [1] Barnett, A.H., Betcke, T.: Stability and convergence of the method of fundamental solutions for Helmholtz problems on analytic domains. *J. Comput. Phys.* **227**, 7003–7026 (2008)
- [2] Buslaev, V.I.: Convergence of multipoint Padé approximants of piecewise analytic functions. *Sb. Math.* **204**, 190–222 (2013)
- [3] Costa, S., Trefethen, L.N.: AAA-least squares rational approximation and solution of Laplace problems. In A. Hujdurović et al., eds., *European Congress of Mathematics*, 511–534 (2023)
- [4] Crowdy, D.G.: Exact solutions to the unsteady two-phase Hele-Shaw problem. *Quart. J. Mech. Appl. Math.* **59** 475–485 (2006)
- [5] Davis, P.J.: *The Schwarz Function and its Applications*. Math. Assoc. Amer. (1974)
- [6] Davis, P.J., Pollak, H.: On the analytic continuation of mapping functions. *Trans. AMS* **87**, 198–225 (1958)
- [7] Driscoll, T. A.: *RationalFunctionApproximation.jl*: Julia software for approximation by rational functions. <https://github.com/complex>

`variables/RationalFunctionApproximation.jl` (2023)

- [8] Driscoll, T.A., Hale, N., Trefethen, L.N.: *Chebfun Guide*. Pafnuty Publications, Oxford (2014)
- [9] Ebenfelt, P., Gustafsson, B., Khavison, D., Putinar, M.: Quadrature domains and their applications. *Oper. Theory Adv. Appl.* **156** (2005)
- [10] Fasondini, M., Hale, N., Spoerer, R., Weideman, J.A.C.: Quadratic Padé approximation: numerical aspects and applications. *Computer Res. Model.* **11**, 1017–1031 (2019)
- [11] Gopal, A., Trefethen, L.N.: New Laplace and Helmholtz solvers. *Proc. Nat. Acad. Sci.* **116**, 10223 (2019)
- [12] Grave, D.-A.: Sur le problème de Dirichlet. *Assoc. Française pour l'Avancement des Sciences, Comptes-Rendus (Bordeaux)* **24**, 111–136 (1895)
- [13] Herglotz, G. Über die analytische Fortsetzung des Potentials ins Innere der anziehenden Massen. *Gekrönte Preisschr. Jablonowkischen Gesellsch. zu Leipzig*, 56 pp. (1914)
- [14] Howison, S.D.: Complex variable methods in Hele-Shaw moving boundary problems. *Euro. J. Appl. Math.* **3**, 209–224 (1992)
- [15] Keller, J.B.: Singularities and Rayleigh's hypothesis for diffraction gratings. *J. Opt. Soc. Am. A* **17** 456–457 (2000)
- [16] MacMillen, D.: `BaryRational.jl`. github.com/macd/BaryRational.jl (2024)
- [17] Millar, R.F.: Singularities and the Rayleigh hypothesis for solutions to the Helmholtz equation. *IMA J. Appl. Math.* **37**, 155–171 (1986)
- [18] Nakatsukasa, Y., Sète, O., Trefethen, L.N.: The AAA algorithm for rational approximation. *SIAM J. Sci. Comput.* **40**, 1494–1522 (2018)
- [19] Nakatsukasa, Y., Trefethen, L.N.: Reciprocal-log approximation and planar PDE solvers. *SIAM J. Numer. Anal.* **59**, 2801–2822 (2021)
- [20] Nehari, Z.: *Conformal Mapping*. McGraw-Hill (1953)
- [21] Newman, D.J.: Rational approximation to $|x|$. *Michigan Math. J.* **11**, 11–14 (1964)
- [22] Schwarz, H.A.: Über die Integration der partiellen Differentialgleichung $\frac{\partial^2 u}{\partial x^2} + \frac{\partial^2 u}{\partial y^2} = 0$ unter vorgeschriebenen Grenz- und Unstetigkeitsbedingungen. *Monatsber. Königl. Akad. Berlin*, 767–795 (1870); see *Gesammelte*

mathematische Abhandlungen, v. 2, AMS (1972)

- [23] Shafer, R.E.: On quadratic approximation. *SIAM J. Numer. Anal.* **11**, 447–460 (1974)
- [24] Shapiro, H.S.: *The Schwarz Function and its Generalization to Higher Dimensions*. Wiley (1992)
- [25] Stahl, H.: The convergence of Padé approximants to functions with branch points. *J. Approx. Th.* **91**, 139–204 (1997)
- [26] Stahl, H.R.: Sets of minimal capacity and extremal domains. arXiv:1205.3811v1 (2012)
- [27] Trefethen, L.N.: Numerical analytic continuation. *Japan J. Appl. Math.* **40**, 1587–1636 (2023)
- [28] Trefethen, L.N.: Polynomial and rational convergence rates for Laplace problems on planar domains. *Proc. Roy. Soc. A* **480**, 20240178 (2024)
- [29] Trefethen, L.N., Wilber, H.D.: Computation of Zolotarev rational functions. Submitted (2024)
- [30] Virtanen, P. et al.: SciPy 1.0: Fundamental algorithms for scientific computing in Python. *Nature Methods* **17**, 261–272 (2020)
- [31] Xue, Y., Waters, S.L., Trefethen, L.N.: Computation of two-dimensional Stokes flows via lightning and AAA rational approximation. *SIAM J. Sci. Comput.* **456**, A1214 (2024)